

Density-matrix renormalization-group study of the disorder line in the quantum axial next-nearest-neighbor Ising model

Matteo Beccaria,¹ Massimo Campostrini,² and Alessandra Feo³

¹*Dipartimento di Fisica and INFN, Università di Lecce, Via Arnesano, 73100 Lecce, Italy*

²*INFN, Sezione di Pisa, and Dipartimento di Fisica "Enrico Fermi" dell'Università di Pisa, Largo Bruno Pontecorvo 3, I-56127 Pisa, Italy*

³*Dipartimento di Fisica, Università di Parma and INFN Gruppo Collegato di Parma, Parco Area delle Scienze, 7/A, 43100 Parma, Italy*

(Received 6 December 2005; published 7 February 2006)

We apply density-matrix renormalization-group methods to study the phase diagram of the quantum axial next-nearest-neighbor Ising model in the region of low frustration where the ferromagnetic coupling is larger than the next-nearest-neighbor antiferromagnetic one. By finite-size scaling on lattices with up to 80 sites we locate precisely the transition line from the ferromagnetic phase to a paramagnetic phase without spatial modulation. We then measure and analyze the spin-spin correlation function in order to determine the disorder transition line where a modulation appears. We give strong numerical support to the conjecture that the Peschel-Emery one-dimensional line actually coincides with the disorder line. We also show that the critical exponent governing the vanishing of the modulation parameter at the disorder transition is $\beta_q=1/2$.

DOI: 10.1103/PhysRevB.73.052402

PACS number(s): 75.10.Jm, 05.10.Cc, 73.43.Nq

The axial next-nearest-neighbor Ising (ANNNI) model is an axial Ising model with competing next-nearest-neighbor antiferromagnetic coupling in one direction. It is a paradigm for the study of competition between magnetic ordering, frustration, and thermal disordering effects. Its phase diagram displays indeed a rich variety of phases. In the most realistic three-dimensional (3D) case, it describes several physical systems from magnetic materials like CeSb to binary alloys or dielectrics like NaNO₂.¹ In the more academic one-dimensional case, it is exactly solvable and several general properties can be rigorously proved about its phase diagram.²

The two-dimensional case is nontrivial and not solvable, but its phase structure is much simpler than in the 3D case. The model is believed to display five phases:³ ferromagnetic $\uparrow\uparrow\uparrow$, antiphase $\uparrow\downarrow\downarrow$, paramagnetic with or without modulation, and floating phase with algebraically decaying spin correlations. This picture is supported by various analytical⁴ and numerical⁵ investigations based on a variety of approximations. However, lacking an exact solution, the precise location of the various transitions is not known beyond approximate treatments. Actually there is no rigorous proof of the existence of all the above phases. In particular the very existence of the floating phase has been recently under debate.⁶

To further simplify the analysis, the 2D case can be studied in the Hamiltonian limit which is a one-dimensional quantum spin $S=1/2$ chain with next-nearest-neighbor coupling. The chain interacts with an external field playing the role of the temperature and triggering phase transitions. The Hamiltonian limit, also called the transverse ANNNI model (TAM) is very interesting in itself, being a simple example where several complicated quantum phase transitions do occur with drastic changes in the qualitative features of the ground state.⁷

The accurate numerical study of the TAM is challenging

notwithstanding its relative simplicity. In this Brief Report we address an open conjecture concerning its disorder line by employing density-matrix renormalization-group methods.

To illustrate the problem, we introduce the TAM Hamiltonian with open boundary conditions, which reads

$$H = -J_1 \sum_{i=1}^{L-1} \sigma_i^z \sigma_{i+1}^z - J_2 \sum_{i=1}^{L-2} \sigma_i^z \sigma_{i+2}^z - B \sum_{i=1}^L \sigma_i^x. \quad (1)$$

We shall present our results in terms of the adimensional ratios $\kappa = -J_2/J_1$ and B/J_1 which are the only parameters that describe the properties of the ground state.

The qualitative phase diagram of the TAM is quite different in the two regions $\kappa < 1/2$ or $\kappa > 1/2$. For $\kappa < 1/2$, the model is in a ferromagnetic phase at low magnetic field B . At $B_{c,1}$, a transition in the Ising class makes the ground state paramagnetic with exponentially decaying spin-spin correlation functions. Further increasing the external field we expect a new transition for $B > B_{c,2} > B_{c,1}$ where the model is still gapped but with a correlation function whose exponential decay has also a spatial modulation. In this phase the asymptotic correlation function in the bulk is conveniently parametrized for large spin separation d by the functional form

$$C^{zz}(d) = \langle \sigma_i^z \sigma_{i+d}^z \rangle \sim c_0 e^{-dr} \cos(\pi qd + \varphi), \quad (2)$$

with r and q being functions of B and κ .

The modulation parameter $q(B, \kappa)$ vanishes at $B = B_{c,2}(\kappa)$ with a certain exponent β_q ,

$$q(B, \kappa) \sim A [B - B_{c,2}(\kappa)]^{\beta_q} \quad \text{as } B \searrow B_{c,2}(\kappa). \quad (3)$$

The critical line $B = B_{c,2}(\kappa)$ is known as a disorder line^{2,8} (see also Ref. 9 for a different definition).

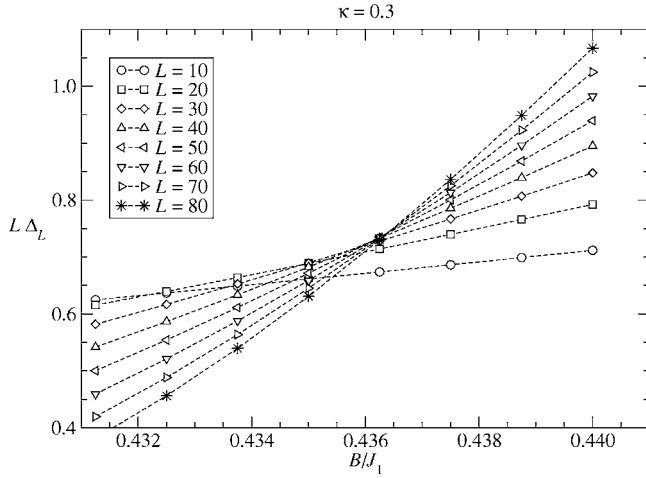


FIG. 1. Finite-size scaling analysis of $L\Delta_L(\kappa, B)$ at $\kappa=0.3$.

The region $\kappa > 1/2$ is much more complicated. At low B the ground state is in a so-called antiphase with typical spin configuration $\uparrow\uparrow\downarrow\downarrow\cdots$. On increasing the magnetic field one expects to observe a first transition to a disordered phase with algebraically decaying C^{zz} (the floating phase) followed by a final transition to the asymptotic paramagnetic phase, i.e., the unique high-temperature phase in the original 2D statistical model. The numerical data in this region are controversial and the size of the floating phase is not clear, being possibly zero.⁶

In this Brief Report, we shall be concerned with the $\kappa < 1/2$ region only. For simplicity, we shall denote this region as the low-frustration region (LFR). In the LFR, there is general consensus about the phase diagram, although only at the qualitative level, i.e., with large variations due to the various approximation employed in its calculation.

Remarkably, the TAM can be solved exactly on a critical line in the LFR, called the Peschel-Emery one-dimensional line (ODL).¹⁰ The spin correlation decays exponentially on the ODL which is immersed in the paramagnetic phase. Little is known analytically of the ODL due to the very tricky nature of the solution. It is still a conjecture that the

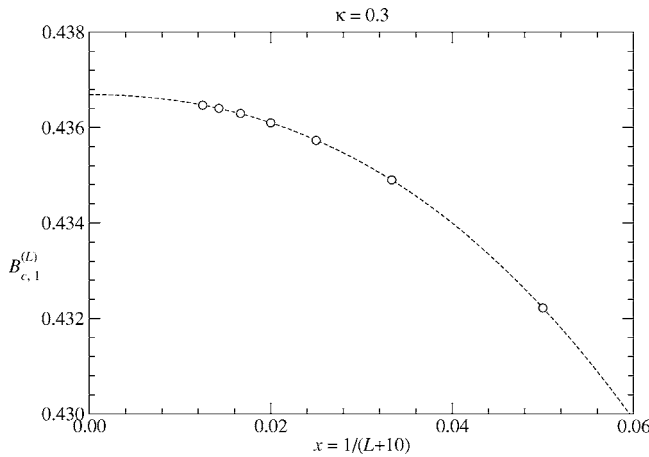


FIG. 2. Extrapolation of the finite-size scaling crossing estimator $B_{c,1}^{(L)}$. $\kappa=0.3$ and $L=10, 20, \dots, 80$.

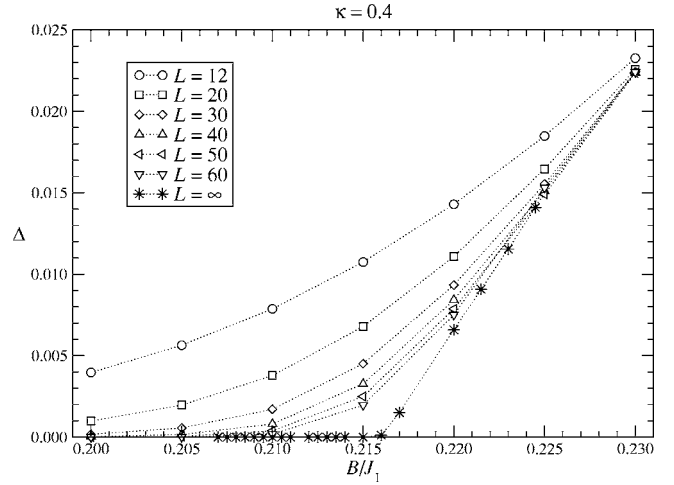


FIG. 3. Finite-size scaling analysis at $\kappa=0.4$. The left plot includes the data obtained with the infinite-size DMRG algorithm and labeled $L=\infty$.

ODL is indeed the disorder line and that therefore

$$B_{c,2}/J_1 = B_c^{PE}/J_1 \equiv \kappa - \frac{1}{4\kappa}. \quad (4)$$

The conjecture is compatible with the numerical simulations of the TAM. However, the agreement $B_{c,2} = B_c^{PE}$ is valid at not more than about 20% accuracy along the line.

The aim of this Brief Report is precisely to give a numerical *proof* with good accuracy of this conjecture. As a by-product we also determine the unknown exponent β_q .

A detailed analysis of the quantum ANNNI model can be found in Ref. 11. The accuracy of the results is poor because of the small considered lattices with fewer than ten sites. Another interesting approach is described in Ref. 12 where an effective Hamiltonian is proposed allowing a considerable reduction of the Hilbert space. Systems up to 32 sites long

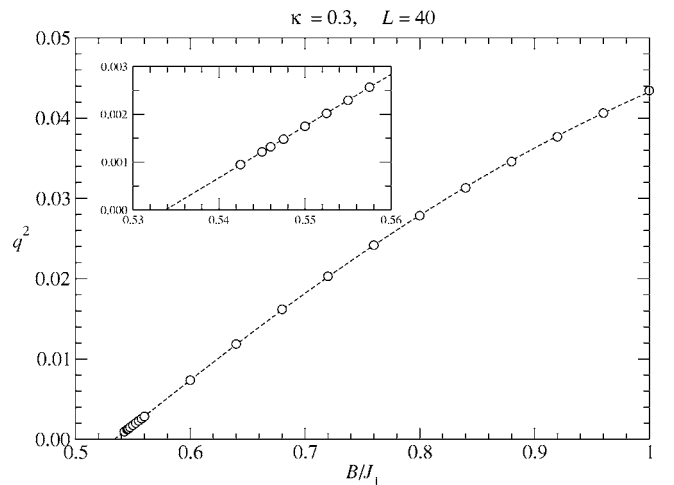


FIG. 4. B dependence of the squared modulation parameter q^2 at $\kappa=0.3$. The fit is performed on the leftmost points near the critical point.

TABLE I. Comparison of the ferromagnetic and disorder critical fields $B_{c,1-2}/J_1$. The DMRG columns are our data. $\tilde{B}_{c,1}$ is obtained from the vanishing of the gap at second order in the magnetic field. The data from Ref. 13 have been interpolated at $\kappa=0.15,0.35$.

κ	$B_{c,1}^{\text{DMRG}}/J_1$	$B_{c,1}/J_1$ (Ref. 13)	$\tilde{B}_{c,1}/J_1$	$B_{c,2}^{\text{DMRG}}/J_1$	$B_{c,2}/J_1$ (Ref. 10)
0.15	0.73405(4)	0.7327(2)	0.74956	1.5168(2)	1.51667
0.20	0.6393(1)	0.6407(4)	0.65336	1.0500(1)	1.05
0.25	0.5403(3)	0.5388(4)	0.55051	0.75001(2)	0.75
0.30	0.43669(4)	0.4368(2)	0.44183	0.53337(5)	0.53333
0.35	0.32821(2)	0.3298(3)	0.32917	0.36428(5)	0.36429
0.40	0.216090(3)	0.2068(3)	0.21548	0.22498(2)	0.225

can be treated, but the approximation is valid only near $\kappa = 1/2$.

A more recent numerical analysis of the LFR is Ref. 13, where the ferromagnetic-paramagnetic Ising transition is analyzed by combining finite-size scaling (FSS) with exact diagonalization of short chains with no more than ten sites.

Here we present a study of the model with higher accuracy and much larger lattices by means of the density-matrix renormalization-group (DMRG) algorithm.¹⁴ Nowadays, this method appears to be the natural choice for one-dimensional quantum spin chains.

We have implemented the finite-size version of the DMRG algorithm computing the two lowest levels $E_{0,1}$ and the energy gap $\Delta = E_1 - E_0$. The algorithm results are very stable when more than 80 states are kept in the block Hamiltonians. In practice the numerical error on Δ is at the level of the machine precision.

For several lattice sizes L of order 10^2 and various frustration ratios κ , we have computed the scaled energy gap $L\Delta_L(\kappa, B)$. The crossing of the associated curves as a function of B at fixed κ is a finite-size estimate of the ferromagnetic critical field $B_{c,1}^{(L)}(\kappa)$. As an example, we show in Fig. 1 our results at $\kappa=0.3$. We have determined the crossing point between the curves associated with a certain L and $L+10$. We expect $B_{c,1}^{(L)} \rightarrow B_{c,1}(\kappa)$ as $L \rightarrow \infty$ with algebraic corrections

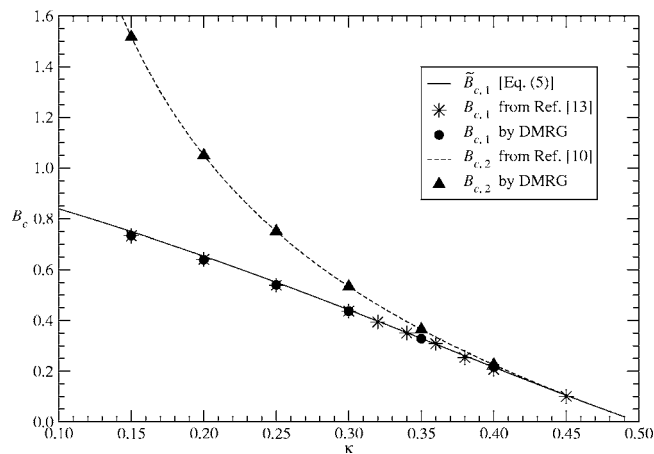


FIG. 5. Phase diagram in the LFR showing the agreement between the disorder line computed with DMRG and the exact one-dimensional line by Peschel-Emery. See Table I for numerical values.

in $1/L$.¹⁵ We show in Fig. 2 the finite-size crossing field plotted as a function of $x = 1/(L+10)$ which is the most convenient variable to extrapolate our $(L, L+10)$ crossings. Indeed, the fitting function $a+bx^2+cx^3$ gives a very good χ^2 of about 10^{-11} . The results for all the considered κ are collected in Table I where we also show (when available) the analogous results from Ref. 13. These are obtained on small lattices crossing L with a fixed $L=4$. This is at most an estimate of $B_{c,1}$. Table I reports also $\tilde{B}_{c,1}$ which is obtained from the vanishing of the gap at second order in B ,¹⁰ and is defined by

$$1 + 2\kappa = \frac{\tilde{B}_{c,1}}{J_1} + \frac{\kappa}{2(1+\kappa)} \left(\frac{\tilde{B}_{c,1}}{J_1} \right)^2. \quad (5)$$

In principle, it is possible to determine $B_{c,1}$ directly in the infinite-size limit by using the infinite-lattice version of the DMRG algorithm. We show in Fig. 3 the result of such a procedure at $\kappa=0.4$. The result for $B_{c,1}$ is fully consistent with the FSS analysis. Also, the exponent $\nu=1$ which governs the vanishing of the mass gap is very clear at $L=\infty$. For the other values of κ we have preferred to avoid the infinite-size algorithm since it is known that it can fail when the phase structure is complicated.¹⁶ From Table I we see that the DMRG estimate $B_{c,1}^{\text{DMRG}}$ and the results of Ref. 13 are globally similar and slightly below the approximation $\tilde{B}_{c,1}$, especially at large $|\kappa-1/2|$. The value from Ref. 13 at $\kappa=0.4$ is somewhat away from the common values of $B_{c,1}^{\text{DMRG}}$ and $\tilde{B}_{c,1}$.

After the determination of the ferromagnetic-paramagnetic Ising transition, we studied $B_{c,2}(\kappa)$ and the critical behavior of the modulation q . We have computed by the DMRG algorithm the spin correlation $C^{\tau\tau}$ on large lattices compared to the correlation length r appearing in Eq. (2). In practice, $L=40$ is enough in all the considered cases. The critical behavior of $q(B)$ is shown in Fig. 4 for $\kappa=0.3$. The vanishing of q^2 is linear in $B-B_{c,2}$. The modulation parameter vanishes with exponent $\beta_q=1/2$. The critical field $B_{c,2}$ coincides with the Peschel-Emery value¹⁰ with high accuracy.

We have repeated the analysis for $\kappa=0.15, 0.2, 0.25, 0.35$, and 0.4 , finding always a very good agreement. The agreement at small frustration is remarkable. From the point of view of the disorder line the next-nearest-neighbor coupling J_2 is a singular perturbation with $B_{c,2} \rightarrow \infty$ in the isotropic

Ising limit $\kappa \rightarrow 0$. We remark that it is nontrivial to extend the calculation of Ref. 10 off the one-dimensional line to prove rigorously that the one-dimensional line is the disorder line. Indeed, the only analytic insight in this direction is the analysis in Ref. 17 where the ODL is proved to be the disorder line, but only mapping the initial $S=1/2$ spin chain into a dual spin $T=1/2$ chain and taking the $T \rightarrow \infty$ limit.

Our results for $B_{c,2}$ are also summarized in Table I together with the Peschel-Emery value. In Fig. 5 we plot the final phase diagram as determined by our DMRG simulations.

In conclusion, we have shown that a DMRG analysis of

the quantum ANNNI model provides strong numerical support to the conjecture that the Peschel-Emery ODL is actually the disorder line. Also, the critical exponent governing the vanishing of the modulation at the disorder transition is $\beta_q=1/2$.

A natural extension of this work concerns the DMRG study of the region $\kappa > 1/2$, which requires much larger lattices to analyze the slow algebraic decay of the spin correlation functions in the would-be floating phase.

We acknowledge conversations with G. F. De Angelis, W. Selke, P. Fendley, and V. Rittenberg.

-
- ¹An old review is by W. Selke, *Phys. Rep.* **170**, 213 (1988). More recent experimental results concerning incommensurate stripe structures in various materials can be found, for instance, in S. Kawano and N. Achiwa, *J. Magn. Magn. Mater.* **52**, 464 (1985); X. Dai, Z. Xu, and D. Viehland, *J. Am. Ceram. Soc.* **78**, 2815 (1995); J. Ricote *et al.*, *J. Phys.: Condens. Matter* **10**, 1767 (1998); D. Viehland, *Phys. Rev. B* **52**, 778 (1995); V. Massidda and C. R. Mirasso, *ibid.* **40**, 9327 (1989); D. Bitko, T. F. Rosenbaum, and G. Aeppli, *Phys. Rev. Lett.* **77**, 940 (1996).
- ²R. Liebmann, *Statistical Mechanics of Periodic Frustrated Ising Systems*, Lecture Notes in Physics Vol. 251 (Springer, Berlin, 1986); J. Stephenson, *Can. J. Phys.* **48**, 1724 (1970); T. Oguchi, *J. Phys. Soc. Jpn.* **20**, 2236 (1965); R. M. Hornreich, R. Liebmann, H. G. Schuster, and W. Selke, *Z. Phys. B* **35**, 91 (1979).
- ³See, for instance, D. Allen *et al.*, *J. Phys. A* **34**, L305 (2001).
- ⁴E. Müller-Hartmann and J. Zittartz, *Z. Phys. B* **27**, 261 (1977); J. Villain and P. Bak, *J. Phys. (Paris)* **42**, 657 (1981); J. Kroemer and W. Pesch, *J. Phys. A* **15**, L25 (1982); M. N. Barber and P. M. Duxbury, *ibid.* **14**, L251 (1981); **15**, 3219 (1982); M. D. Grynberg and H. Ceva, *Phys. Rev. B* **36**, 7091 (1987); M. A. S. Saqi and D. S. McKenzie, *J. Phys. A* **20**, 471 (1987); Y. Murai, K. Tanaka, and T. Morita, *Physica A* **217**, 214 (1995).
- ⁵W. Selke and M. E. Fisher, *Z. Phys. B: Condens. Matter* **40**, 71 (1980); W. Selke, *ibid.* **43**, 335 (1981); A. Sato and F. Matsubara, *Phys. Rev. B* **60**, 10316 (1999).
- ⁶T. Shirahata and T. Nakamura, *Phys. Rev. B* **65**, 024402 (2002).
- ⁷See, for instance, D. V. Shopova and D. Uzunov, *Phys. Rep.* **379**, 1 (2003) or the recent book by S. Sachdev, *Quantum Phase Transitions* (Cambridge University Press, Cambridge, UK, 2001).
- ⁸J. Stephenson, *Phys. Rev. B* **1**, 4405 (1970).
- ⁹K. Binder, W. Kinzel, and W. Selke, *Surf. Sci.* **125**, 74 (1983).
- ¹⁰I. Peschel and V. J. Emery, *Z. Phys. B: Condens. Matter* **43**, 241 (1981).
- ¹¹C. M. Arizmendi, A. H. Rizzo, L. N. Epele, and C. A. Garcia Canal, *Z. Phys. B: Condens. Matter* **83**, 273 (1991); P. Sen, S. Chakraborty, S. Dasgupta, and B. K. Chakrabarti, *ibid.* **88**, 333 (1992).
- ¹²H. Rieger and G. Uimin, *Z. Phys. B: Condens. Matter* **101**, 597 (1996).
- ¹³Paolo R. Colares Guimares, J. A. Plascak, F. C. S. Barreto, and J. Florencio, *Phys. Rev. B* **66**, 064413 (2002).
- ¹⁴S. R. White, *Phys. Rev. Lett.* **69**, 2863 (1992); *Phys. Rev. B* **48**, 10345 (1993). A complete updated bibliography of applications of the DMRG can be found in the recent review by U. Schollwöck [*Rev. Mod. Phys.* **77**, 259 (2005)], and at the web site <http://quattro.phys.sci.kobe-u.ac.jp/dmrg.html>
- ¹⁵C. J. Hamer and M. N. Barber, *J. Phys. A* **14**, 259 (1981).
- ¹⁶U. Schollwöck, S. Chakravarty, J. O. Fjærestad, J. B. Marston, and M. Troyer, *Phys. Rev. Lett.* **90**, 186401 (2003).
- ¹⁷D. Sen, *Phys. Rev. B* **43**, 5939 (1991).